Supplementary Information (SI) for Journal of Materials Chemistry A.
This journal is © The Royal Society of Chemistry 2025

Assessing the Role of Morphological Changes as the Origin of Improved Cycling Stability of Sn-based Anodes for Sodium-ion Batteries

Carla Albenga[1], James A. Gott[1], Amalie Skurtveit[2], Jason M. Warnett[1], Faduma M. Maddar[1], Alexey Y. Koposov[2,3], Gustavo Pinzón[4], Geoff West[1], Ivana Hasa[1*]

[1] *WMG, University of Warwick Coventry, CV4 7AL, United Kingdom*

[2] *Centre for Materials Science and Nanotechnology, Department of Chemistry, University of Oslo, Blindern, 0315 Oslo, Norway*

[3] *Department of Battery Technology, Institute for Energy Technology (IFE), 2007 Kjeller, Norway*

[4] *European Synchrotron Radiation Facility, Grenoble, France*

*** Corresponding author**: ivana.hasa@warwick.ac.uk

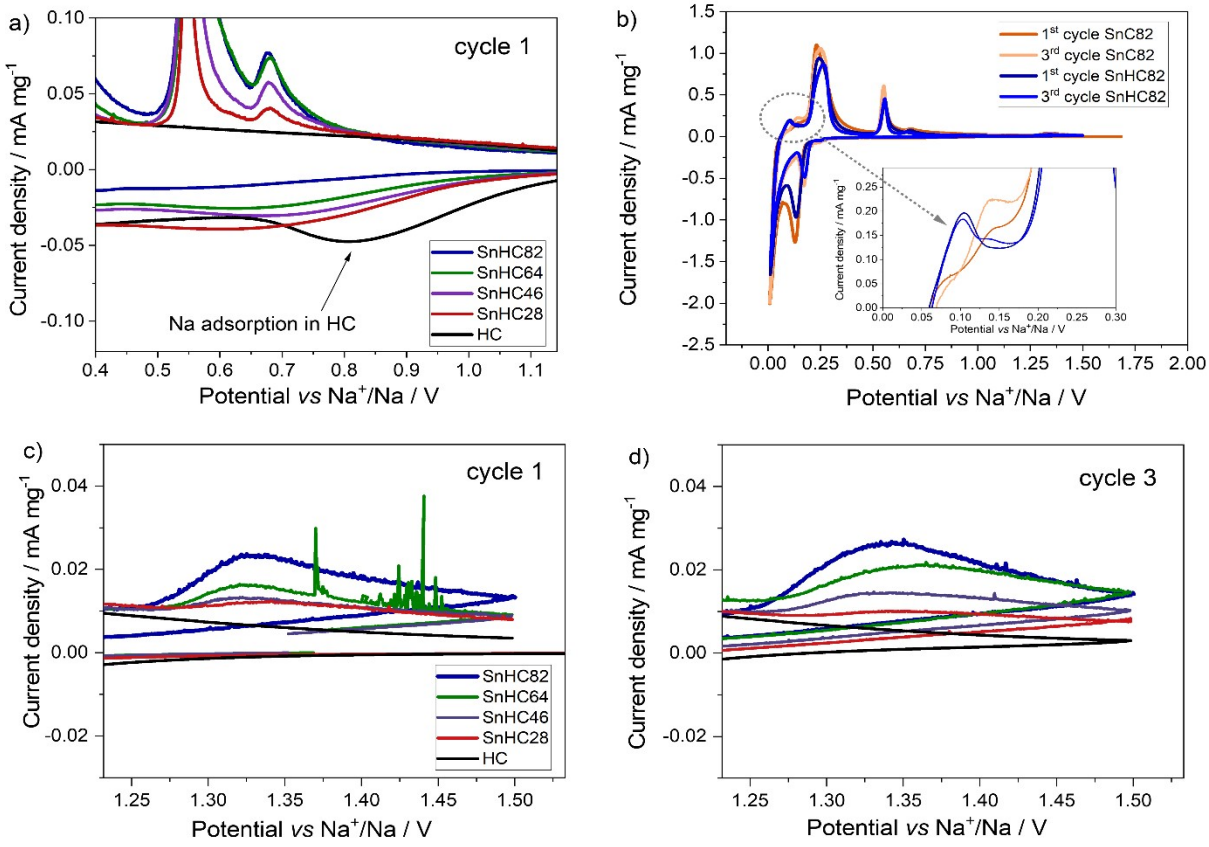

Fig. S1 a) Cyclic voltammetry of the Sn:Carbon black (8:2), *i.e.* SnC82 electrode, using 1 M $NaPF_6$ in diglyme as electrolyte. Zoomed region of CV tests reported in Figure 1 a), highlighting **b)** electrolyte decomposition at ~1.3 V in Sn/HC based electrodes, **c)** Na adsorption in HC at ~0.8 V at cycle 1.

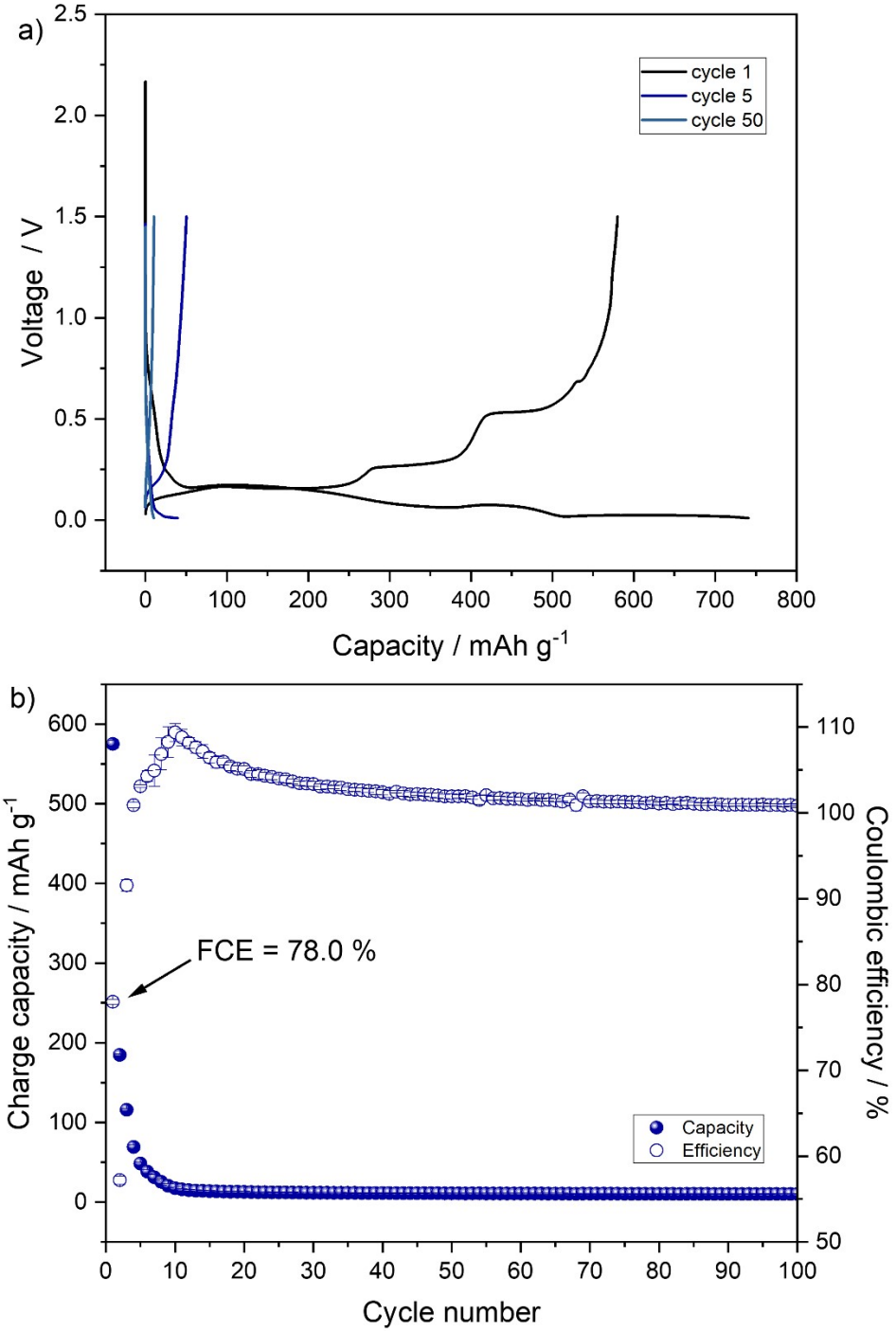

Fig. S2 Galvanostatic cycling tests of micrometric Sn:HC (80:20 wt.%), i.e. SnHC82, using 1M $NaPF_6$ in EC:DEC 3 : 7 (v/v%) as electrolyte. **a)** Voltage profile during galvanostatic cycling at 50 mA g^{-1} (1st cycle) and 100 mA g^{-1} (5th and 50th cycle) and corresponding **b)** cycling stability in terms of charge (de-sodiation) capacity and Coulombic efficiency.

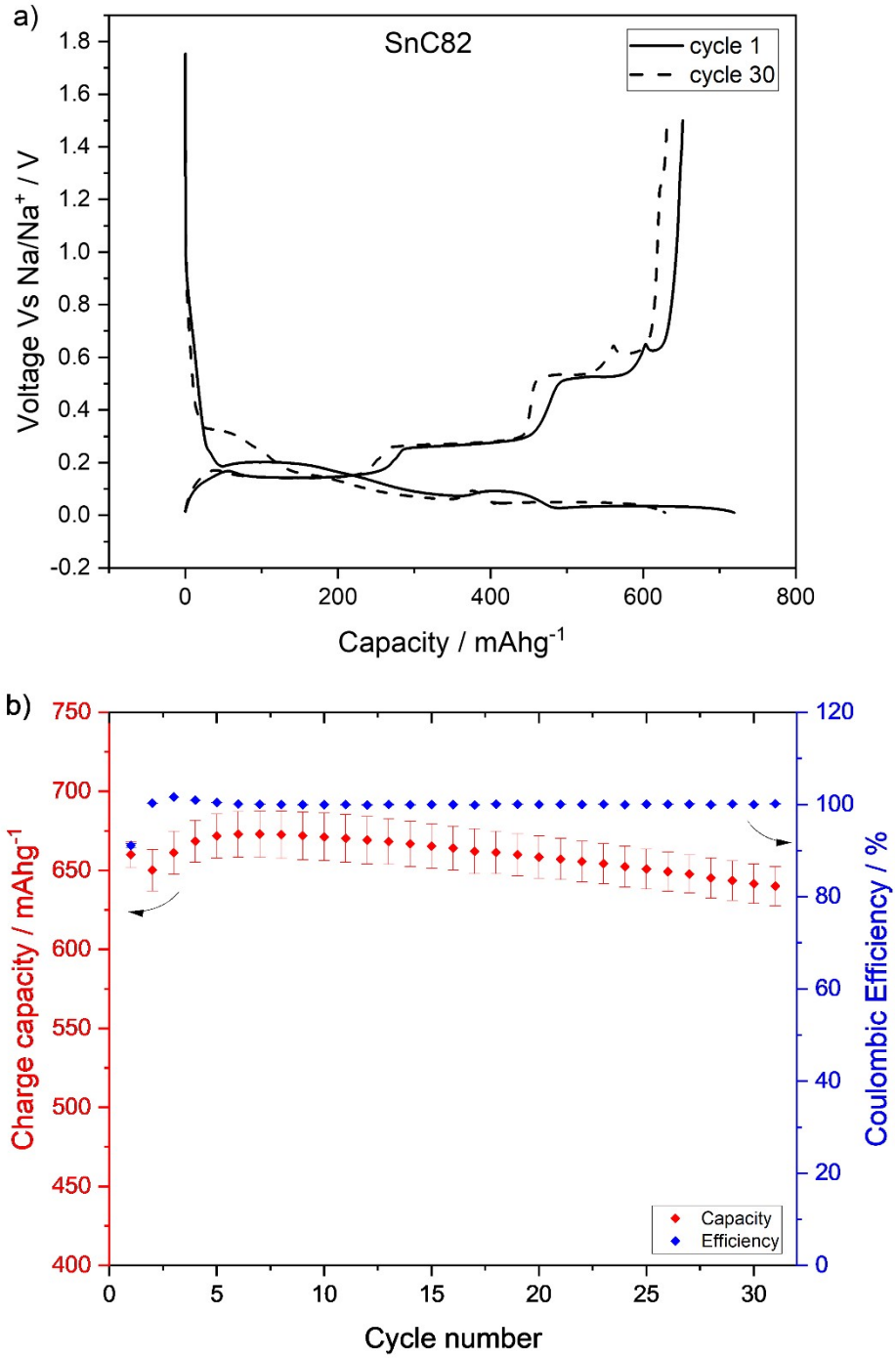

Fig. S3 Galvanostatic cycling tests of Sn:Carbon black (8:2), *i.e.* SnC82, using 1 M $NaPF_6$ in diglyme as electrolyte. **a)** Voltage profile during galvanostatic cycling at 50 mA g^{-1} (1^{st} cycle) and 100 mA g^{-1} (30^{th} cycle) and corresponding **b)** cycling stability and Coulombic efficiency.

Calculation of theoretical capacity:

The theoretical capacity for the Sn/HC composite electrodes was calculated using the following equation:

$C_{th(Sn:HC)} = C_{th,Sn} * \%wt_{Sn} + C_{exp,HC} * \%wt_{HC} + C_C * \%wt_C$

With:

$*C_{th,Sn}$= 847 mAh g^{-1} (theoretical capacity of Sn)

$** C_{exp,HC}$= 295 mAh g^{-1} (reversible HC capacity obtained at 50 mA g^{-1} in Na half-cell)

$***C_C$=180 mAh g^{-1} (reversible capacity of carbon black from [1])

The wt.% is calculated considering that 80% of Sn in the active material corresponds to 72% of Sn in the total electrode composition, but the active components in the electrode composition correspond to the 95% of the total composition (90% of active material, 5% of carbon black and 5% binders).

The overall calculated values are calculated as follows:

$C_{th(SnHC82)} = 847 * 0.7579 + 295 * 0.1895 + 180 * 0.0526 = 707.31$ mAh g^{-1}

$C_{th(SnHC64)} = 847 * 0.5684 + 295 * 0.3789 + 180 * 0.0526 = 602.68$ mAh g^{-1}

$C_{th(SnHC46)} = 847 * 0.3789 + 295 * 0.5684 + 180 * 0.0526 = 498.07$ mAh g^{-1}

$C_{th(SnHC28)} = 847 * 0.1895 + 295 * 0.7579 + 180 * 0.0526 = 393.56$ mAh g^{-1}

$C_{th(SnCB82)} = 847 * 0.7579 + 180 * (0.1895 + 0.0526) = 685.52$ mAh g^{-1}

[1] T. Palaniselvam, C. Mukundan, I. Hasa, A. L. Santhosha, M. Goktas, H. Moon, M. Ruttert, R. Schmuch, K. Pollok, F. Langenhorst, M. Winter, S. Passerini, P. Adelhelm, Assessment on the Use of High Capacity "Sn4P3"/NHC Composite Electrodes for Sodium-Ion Batteries with Ether and Carbonate Electrolytes. Adv. Funct. Mater. 2020, 30, 2004798.

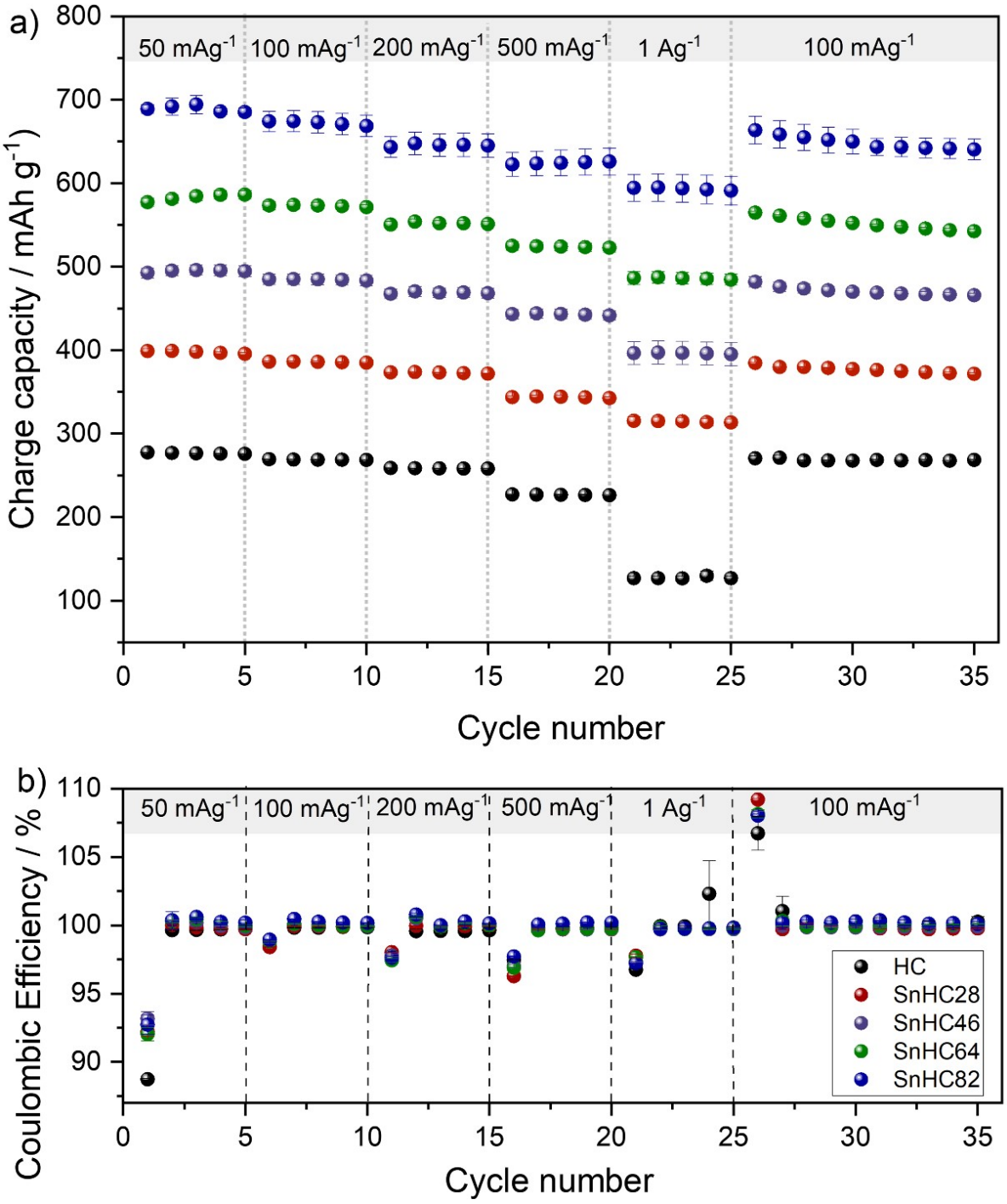

Fig. S4 Rate capability tests at different current densities reported in terms of a) cycling response and b) Coulombic Efficiency for the Sn/HC and pure HC electrodes. Tests conducted at 25 °C within the 0.01-1.5 V range. Electrolyte: 1 M $NaPF_6$ in diglyme.

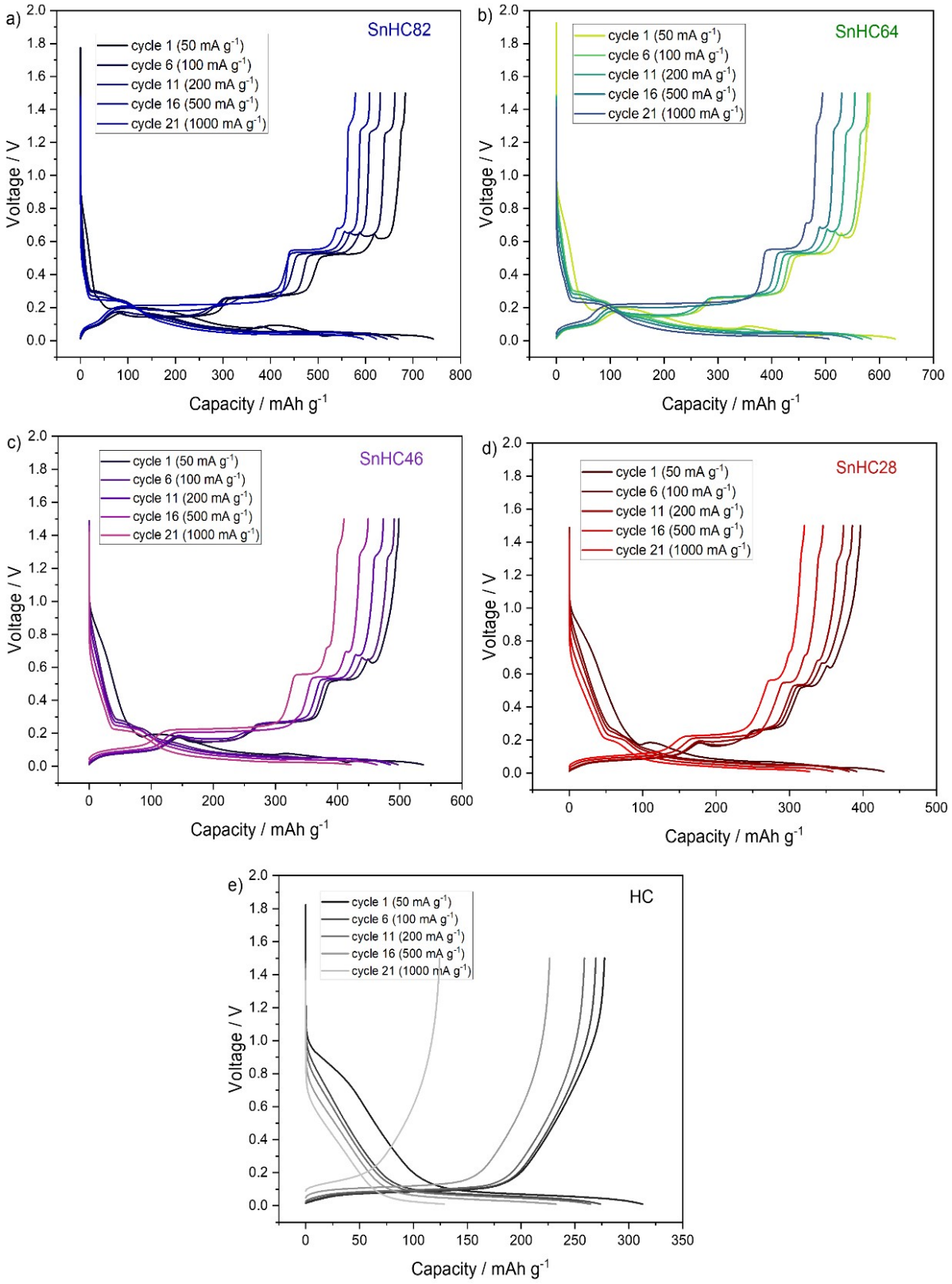

Fig. S5 Voltage profiles of Sn/HC electrodes and pure HC obtained during the rate capability tests shown in Figure S4. Tests conducted at 25 °C within the 0.01-1.5 V range. Electrolyte: 1 M $NaPF_6$ in diglyme.

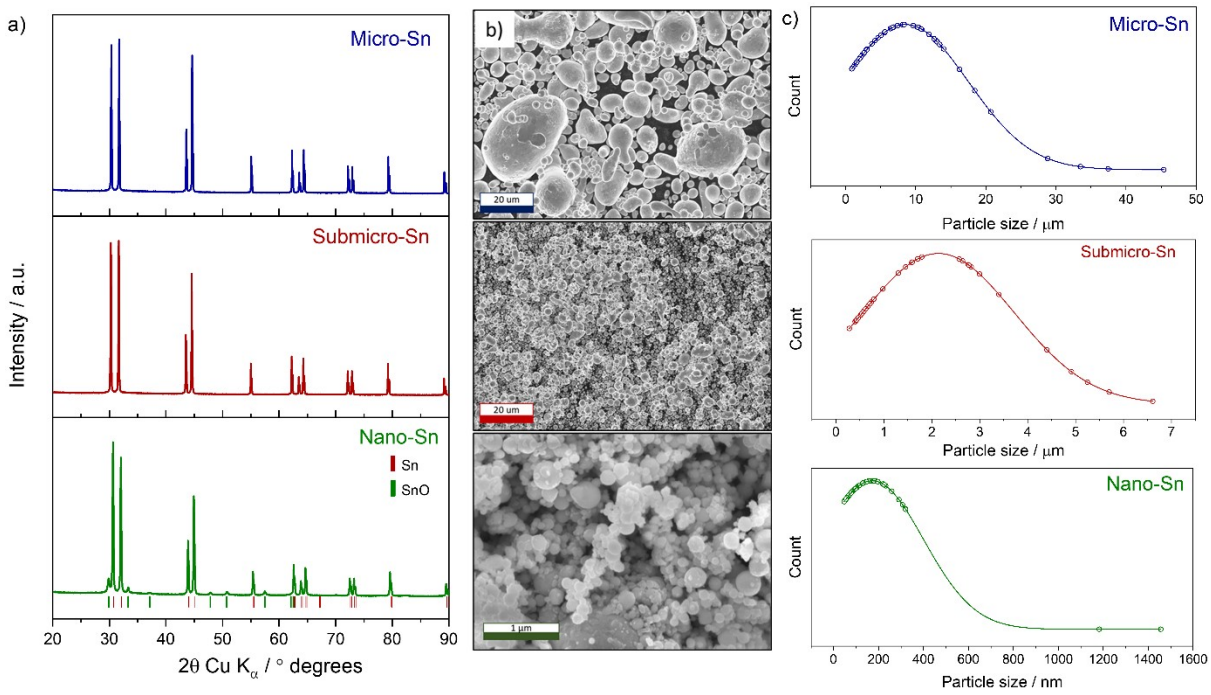

Fig. S6 a) XRD pattern of the as received Sn powders. b) SEM images of the pristine Sn powders as received. **c)** Particle size distribution of micrometric, submicrometric, and nanometric Sn powder as received. The particle size analysis was carried out using the software ImageJ and the SEM images of the pristine powders.

Table S1 Analysis of XRD patterns reported in Fig. S6 a) for micrometric, submicrometric, and nanometric Sn particles.

XRD peak analysis	**Micro-Sn**	**Submicro-Sn**	**Nano-Sn**
Peak 1 position	30.3°	30.3°	30.3°
Peak 2 position	31.7°	31.7°	31.7°
FWHM (peak1 = peak2)	0.15°	0.16°	0.19°
Area(Peak1)/Area(Peak2)	0.95	0.99	1.08

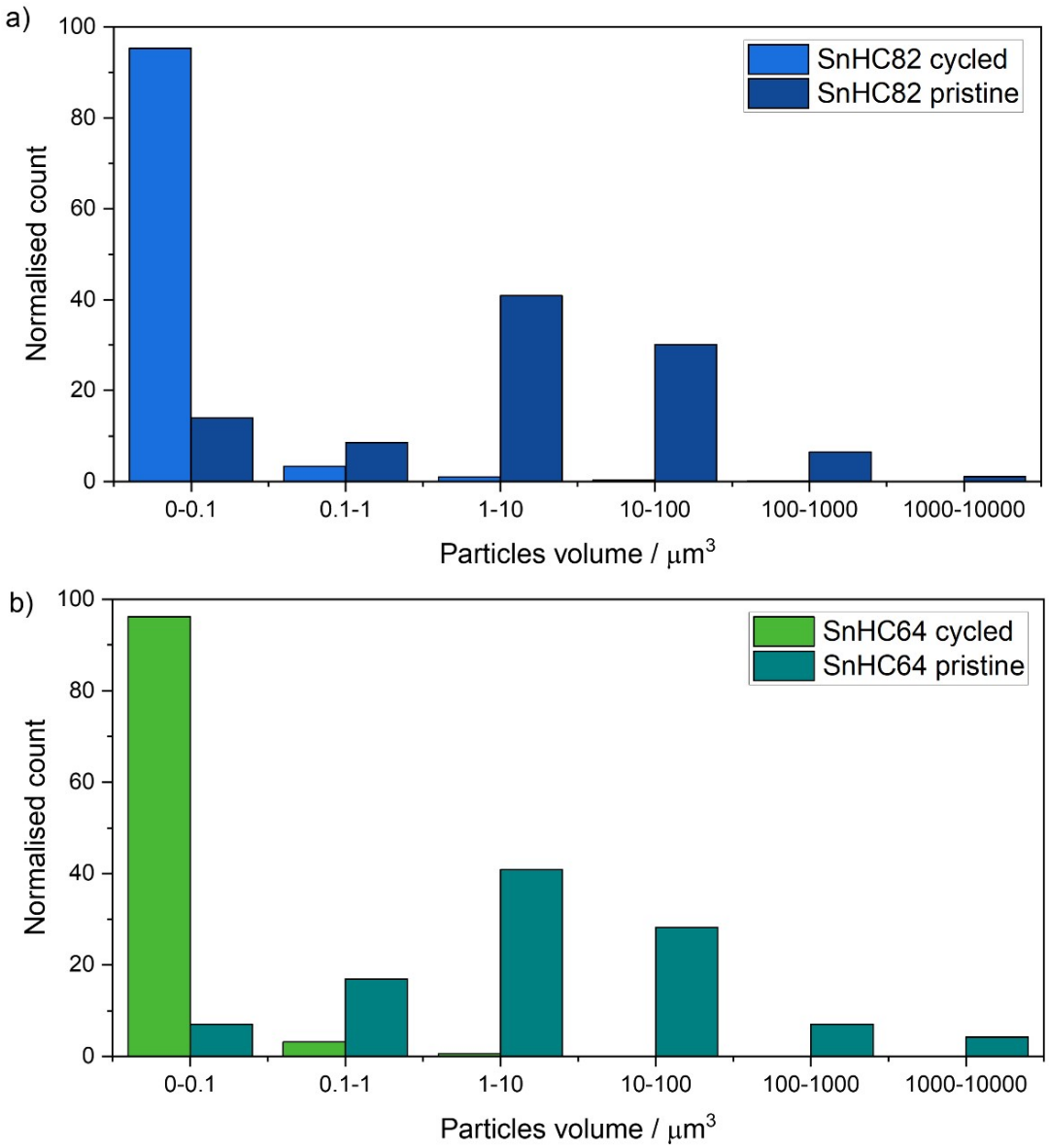

Fig. S7 Particle size distribution of the pristine and cycled (25 cycles) **a)** SnHC82 and **b)** SnHC64 electrodes calculated from Phase Contrast XCT (30 nm resolution images).

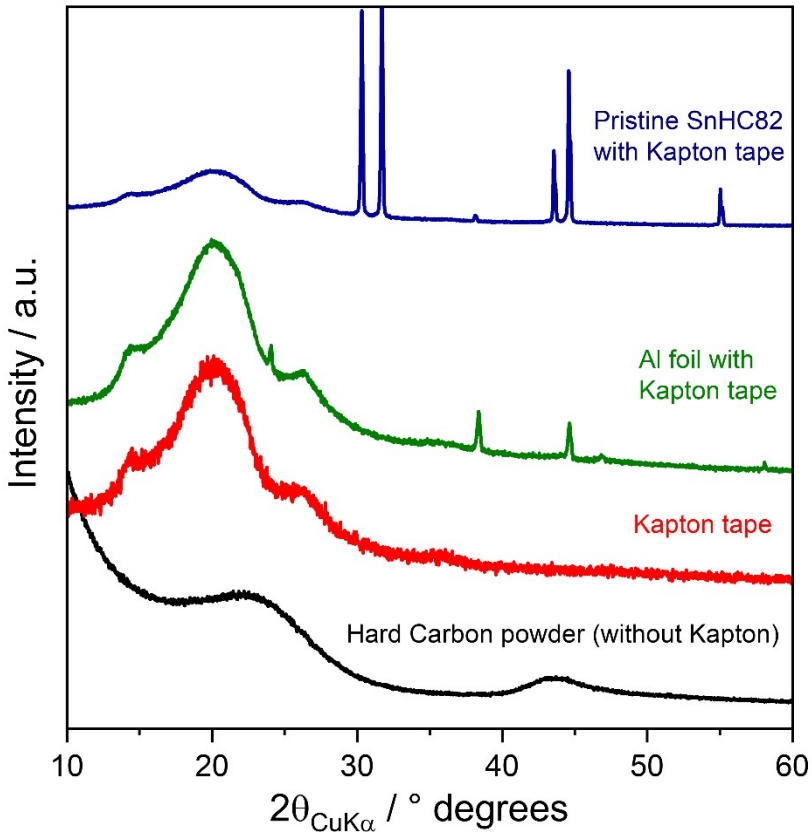

Fig. S8 XRD measurements conducted to confirm Kapton tape contrbution on Fig. 6 a). The data provide a comparison of the XRD patterns for HC powder, Kapton tape, the aluminium current collector with Kapton tape, and the electrodes with Kapton tape. This comparison confirms that the dominant feature at low angles in Fig 6 a) is primarily due to the Kapton tape

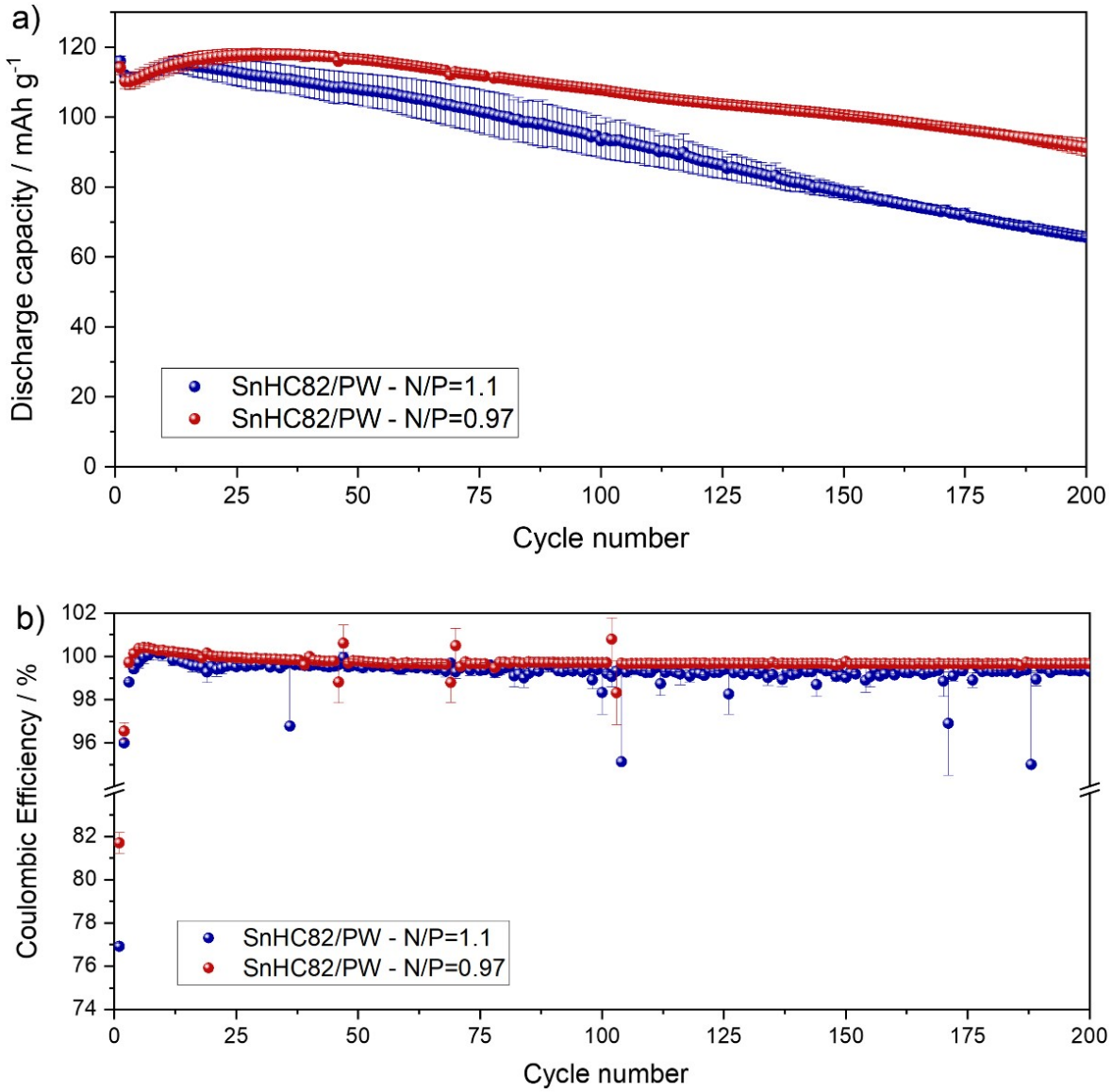

Fig. S9 a) Galvanostatic cycling in terms of discharge capacity and **b)** Coulombic efficiency of SnHC82-PW full cells with N/P ratio of 1.1 and 0.97 cycled at 50 mA g^{-1} for the 1st cycle and 100 mA g^{-1} for the following cycles within a voltage range of 1.3-3.8 V. Tests conducted at 25 °C. Electrolyte: 1 M $NaPF_6$ in diglyme.

Videos provided as separate file in Supporting Information: 3D FIB-SEM tomography of 200 µm wide 100 µm deep volume trench cuts were made using a 30 kV 28 nA Ar beam. Slices (nominal thickness of 75 nm) were generated and imaged. The aligned images are shown in the video links below.